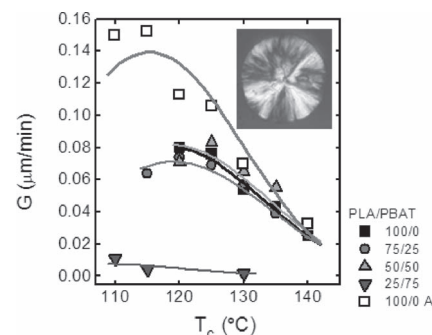


Isothermal Cold-Crystallization of PLA/PBAT Blends With and Without the Addition of Acetyl Tributyl Citrate

Enic Quero, Alejandro J. Müller,* Francesca Signori, Maria-Beatrice Coltelli, Simona Bronco

The isothermal cold-crystallization kinetics of the PLA phase is studied by DSC and the crystallization from the melt by PLOM. Even though the blends exhibit two phases by SEM, several pieces of evidence indicate that partial miscibility may be present in these blends: small changes in both T_g and T_m of the PLA phase; a dependence of the spherulitic growth rate on blend composition and the occlusion of PBAT droplets inside PLA spherulites. Acetyl tributyl citrate is able to plasticize both phases in the blends, but it displays a preference to dissolve within the PBAT rich phase. There is a synergistic effect on the increase in the overall crystallization rate of the PLA rich phase when both ATBC and PBAT are present in the blend.



1. Introduction

The thermal properties of biodegradable poly(lactic acid) (PLA)/poly(butylene adipate-co-terephthalate) (PBAT) blends have received some attention in the recent literature. Even though the blends form two phases as reported by various authors,^[1,2] partial miscibility has also been recently claimed since a DSC study reported a decrease of 4 °C in the glass transition temperature (T_g) of PLA when the blend contains 60% by weight PBAT.^[3]

The objective of obtaining blends such as those studied in this work is to enhance the properties of PLA. PLA is a biodegradable polymer that has excellent mechanical resistance, but it is very brittle.^[4] Many attempts to lower its brittleness have been reported in the literature, mostly by copolymerization with a flexible copolymer, plasticization, or addition of a flexible dispersed phase. The addition of a plasticizer to PLA has been extensively studied, especially regarding mechanical properties;^[5–9] an enhancement and an increase in elongation at break is obtained as a consequence of the plasticization process. Recent studies of Xiao et al.^[10] have shown that the addition of triphenyl phosphate as a plasticizer increases the spherulitic growth rate of PLA, as well as decreases the equilibrium melting temperature (T_m^0) as an effect of the plasticization of the chains. Previous work of Coltelli et al.^[1] showed the plasticizing effect of acetyl tributyl citrate (ATBC), which can induce a decrease in T_g and an improvement in the mechanical properties of PLA/PBAT blends.

PLA has also been blended with a flexible phase and several properties of these blends have been reported. Tsuji et al.^[11] studied the thermal behavior of poly(L-lactic acid) (PLLA)/poly(D-lactic acid) (PDLA) blends, with

E. Quero, A. J. Müller
Grupo de Polímeros, Universidad Simón Bolívar,
Caracas 1080-A, Venezuela
Fax: 58(212)9063388
E-mail: amuller@usb.ve

F. Signori, S. Bronco
Istituto per i Processi Chimico-Fisici (IPCF-CNR UOS Pisa),
Area della Ricerca, Via G. Moruzzi 1, 56124 Pisa, Italy
M.-B. Coltelli
Dipartimento di Chimica e Chimica Industriale dell'Università
di Pisa, Via Risorgimento 35, 56126 Pisa, Italy
M.-B. Coltelli
SPIN-PET s.r.l., Via Rinaldo Piaggio 32, 56025 Pontedera (Pisa), Italy

a proportion of PDLA up to 10%. They found that PDLA has a nucleating effect on the crystallization of the PLLA phase when present in a percentage greater than 1%. Shibata et al.^[12] studied the properties of PLLA blended with poly(butylene succinate-co-l-lactate) (PLLA/PBSL) and poly(butylene succinate) (PLLA/PBS), observing a two-phase morphology with partial miscibility as evidenced by the decrease in the T_g of the PLLA fraction and the increase in T_g of the PBS and PBSL fractions. Yeh et al.^[13] studied the properties of PLA blended with poly(ϵ -caprolactone) (PLA/PCL), and deduced by DMA testing that they are partially miscible; in addition, the PCL phase increases the crystallization rate of the PLA fraction. In the case of the PLA/PCL blends, several studies of the mechanical properties show little improvement in the elongation at break.^[14–17]

Reactivity and structural change occurring in polyesters in the melt can also affect thermal properties. The processing of PLA and PBAT can slightly modify the molecular weight as evidenced by Signori et al.^[18] inducing degradation of polyesters as a function of experimental conditions. Moreover, the trans-esterification during blending between the two polyesters is reported to alter the macromolecular structure improving compatibility, but these reactions were found to only slightly affect the macromolecular structure in the absence of proper trans-esterification catalysts and with reduced blending time.^[19]

The main objective of the present work is to study the isothermal crystallization of the PLA component within PLA/PBAT blends and the influence of ATBC as a plasticizer on the thermal properties of the blends.

2. Experimental Section

2.1. Materials

Two commercial, biodegradable polymers were used to obtain the blends: PLA (NatureWorks, PLA 2002D) and the random copolymer PBAT (BASF, Ecoflex F BX 7011). The polymers had number-average molecular weights of 200 000 and 55 000 g mol⁻¹, respectively. ATBC (Aldrich, Milan), 98% pure, was used as received.

2.2. Preparation of Blends

The blends were prepared using a Brabender OGH47055 internal mixer. The mixing process was carried out at a temperature of 200 °C during a 10 min cycle with a 50 rpm screw rotation rate, by purging nitrogen gas during mixing to prevent degradation of the polymers.^[18] The PLA/PBAT blends were prepared in the following weight/weight proportions: 0/100, 25/75, 50/50, 75/25, 100/0. Another set of blends was prepared by adding 10% by weight of ATBC, hence the following PLA/PBAT/ATBC

blends were prepared: 0/100/10, 25/75/2.5, 50/50/5, 75/25/7.5, 100/0/10, they are denoted 0/100A, 25/75A, 50/50A, 75/25A, 100/0A.

All test samples were obtained by compression molding at 180 °C using a 6 min molding cycle followed by quenching in a mixture of water and ice.

The absence of degradation and trans-esterification reactions during blend preparation was verified by FTIR and size exclusion chromatography (SEC) experiments (not shown here).

2.3. Scanning Electron Microscopy (SEM)

The morphology of the blends was observed using a JEOL JSM-6390 microscope. The samples were previously fractured after immersion in liquid nitrogen for 30 minutes and sputtered with gold powder in order to obtain an adequate contrast for the SEM observations. An acceleration voltage of 25 kV was used for all observations.

2.4. Differential Scanning Calorimetry (DSC) Analysis

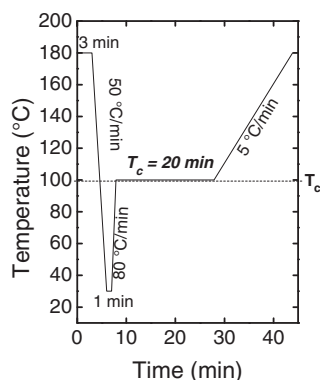
Samples of 10 mg were encapsulated in aluminum pans and measured using a Perkin Elmer DSC-7 calorimeter under an inert atmosphere of ultra high purity N₂. Calibration of the equipment was performed using indium and tin. Standard and isothermal scans were carried out as described below.

2.4.1. Standard DSC Experiments

Standard DSC experiments were carried out with a heating and cooling rate of 5 °C min⁻¹, within the range of 10 and 180 °C. The thermal history of the samples was erased at 180 °C for 3 min, after a first controlled heating scan from 25 °C. The enthalpies of crystallization and melting were normalized according to the proportion of the components in the blends.

2.4.2. Isothermal DSC Experiments (Isothermal Cold-Crystallization)

Isothermal crystallization of the PLA component was carried out after erasing the thermal history of the samples for 3 min at 180 °C. The samples were quickly cooled from the melt to the glassy state at a cooling rate of 50 °C min⁻¹ and then rapidly heated to the cold crystallization temperature (T_c) at a heating rate of 80 °C min⁻¹. The sample was kept at the T_c for 20 min and then heated from T_c to 180 °C at 5 °C min⁻¹. Both isothermal crystallization and later controlled heating scans were recorded. Figure 1 shows the method employed to perform the isothermal cold-crystallization experiments. This method was chosen because the crystallization of the PLA fraction from the melt was very slow, hence, the samples failed to crystallize from the melt without considerable thermal degradation of the material. Employing the method depicted in Figure 1 substantially accelerated the overall crystallization (as compared to the isothermal crystallization from the melt), since the method promotes the nucleation of PLA during the previous cooling and subsequent heating from the glassy state. The enhanced nucleation was



■ Figure 1. Thermal program used for isothermal scans.

verified by a dramatic reduction in spherulitic size as compared to melt crystallized PLA (results not shown).

2.5. Dynamic-Mechanical Analysis (DMA)

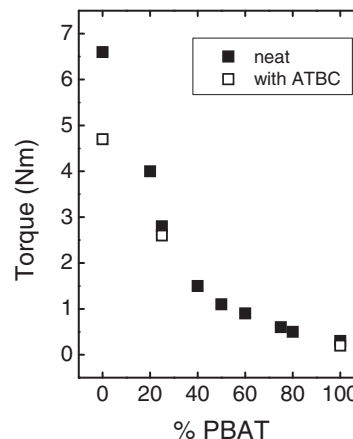
DMA was carried out using a Rheometrics, RSA II solids analyzer, in order to measure the glass transition temperature of the blends. The samples were measured at a constant strain of 0.05 in order to remain within the linear viscoelastic range. A heating rate of 3 °C min⁻¹ was used, with a cyclic stress frequency of 0.03 s⁻¹. The dual cantilever geometry was used in these experiments and the samples were compression molded bars with a thickness of 1.5 mm, following the molding procedure previously described.

2.6. Polarized Light Optical Microscopy (PLOM)

The spherulite growth rate experiments were performed by recording the growth of spherulites in a Leica DM 2500P polarized light optical microscope. Samples with a thickness of less than 1 μm were crystallized from the melt by cooling to T_c at a rate of 90 °C min⁻¹, after erasing the thermal history at 180 °C for 3 min. A temperature controlled heating plate (Linkam, TP 91) was used for these experiments and the dimensions of the spherulites were periodically registered with a Leica DFC 280 digital camera. Pictures were taken every 10–120 s depending on the apparent superstructural growth rate observed in the microscope. The plots of spherulite radius versus time were linear in all cases and their slope was taken as the spherulitic growth rate. The reported spherulite growth rates are averages of at least three different spherulite growth experiments.

3. Results and Discussion

The final torque measured during the mixing process is shown in Figure 2. Thermal-oxidative degradation was prevented by a nitrogen flow inside the mixing chamber. The blends with ATBC have slightly lower torque values, as a consequence of its plasticizing effect. In the case of neat PLA the plasticizing effect



■ Figure 2. Final mixing torque values of the PLA/PBAT blends.

of ATBC caused a more noticeable reduction in torque values. Figure 2 also shows that the addition of PBAT decreases the final torque, which indicates a lower melt viscosity.

The blends showed a two-phase morphology, as can be seen in Figure 3, in accordance to what was previously reported by Coltelli et al.^[1] For all blend compositions shown in Figure 3, the minor phase, whether it was PLA or PBAT, was dispersed in the matrix as droplets, which is very common in two-phase systems with largely different melt viscosities. Nevertheless, this should not be taken as a definite statement about the miscibility of the blends, since they could be partially miscible, as will be evidenced below. The interphase is well defined in the blends with and without plasticizer, which is indicative of low adhesion between the PLA rich and PBAT rich phases.

Figure 4 shows the second DSC heating scans of the PLA/PBAT blends. The values of the glass transition temperature (T_g), the peak temperatures of the cold-crystallization exotherm and melting endotherm (T_{cc} and T_{m} , respectively) of the PLA rich phase, as well as the cold crystallization and melting enthalpies (ΔH_{cc} and ΔH_{m} , respectively) are shown in Table 1. These reported values were registered from the second heating scan of the samples, which was the third step in the standard DSC experiments. The first step was a controlled heating scan prior to erasing of the thermal history of the material, while the second step was a controlled cooling scan down to 10 °C. The cooling scans of the samples did not show any crystallization exothermal peaks for the PLA rich phase.

The melting behavior of the PBAT rich phase could not be studied in the blends because its broad melting peak is located within the cold-crystallization temperature range of the PLA rich phase. The latent enthalpy of fusion for the PBAT rich phase was smaller than that of PLA rich

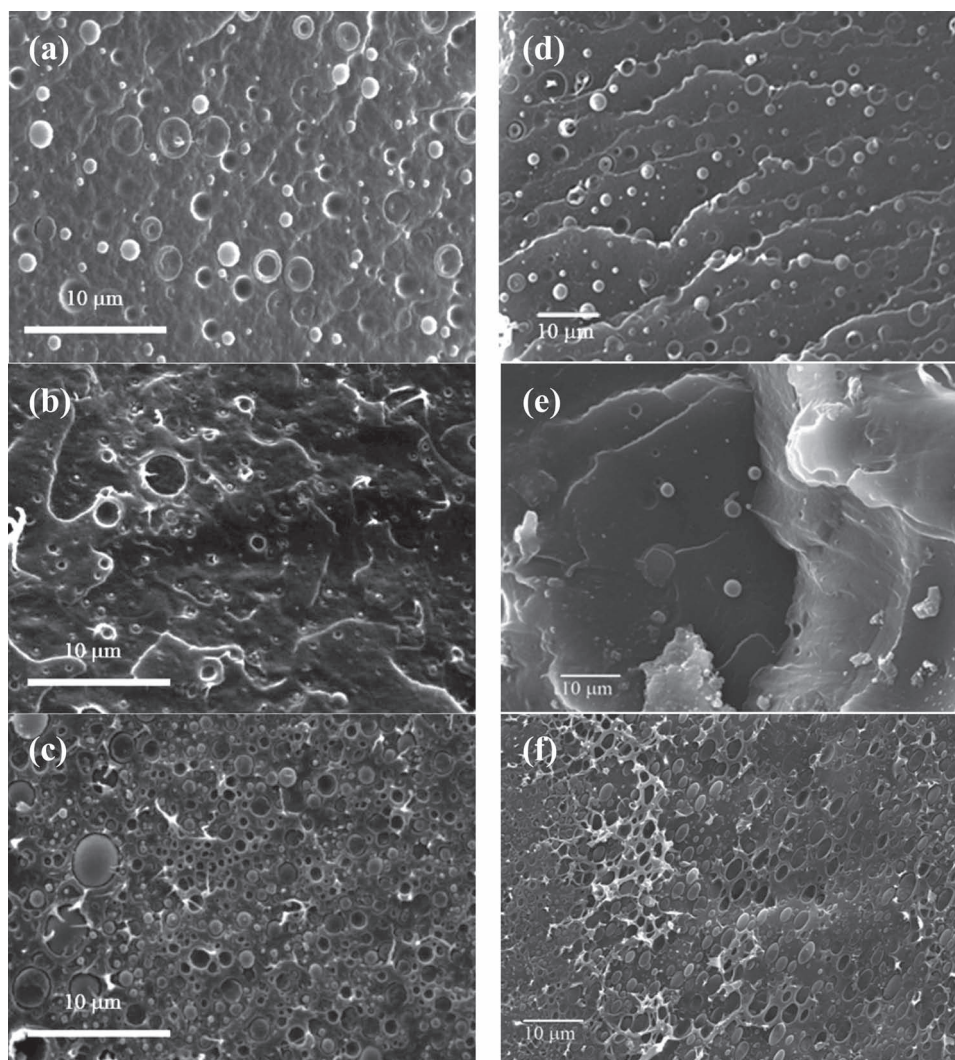


Figure 3. SEM micrographs of the PLA/PBAT blends. Blends without additives: 25/75 (a), 50/50 (b) and 75/25 (c). With ATBC: 25/75A (d), 50/50A (e) and 75/25A (f).

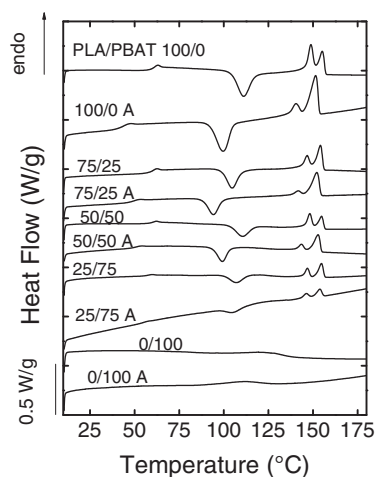


Figure 4. DSC heating scans of the PLA/PBAT blends.

phase. The degree of crystallinity of the PLA phase was determined according to Equation 1:

$$X_c = \frac{\Delta H_m - \Delta H_{cc}}{\Delta H_{m100\%}} \quad (1)$$

where X_c is the degree of crystallization, ΔH_m is the normalized melting enthalpy according to the PLA proportion in the blends, ΔH_{cc} is the cold-crystallization enthalpy of the PLA, and $\Delta H_{m100\%}$ is the melting enthalpy of the 100% crystalline PLA. The value of ΔH_{cc} is affected when there is overlap with the latent heat of melting of the PBAT phase, hence it could be underestimated leading to errors in the crystallinity degree calculated with Equation 1.

■ Table 1. Thermal properties on second heating DSC scans of the PLA/PBAT blends.

PLA/PBAT	T_g 1/2 C_p [°C] ^{a)}	T_{cc} [°C] ^{a)}	ΔH_{cc} [J g ⁻¹] ^{a)}	T_m [°C] ^{a)}	ΔH_m [J g ⁻¹] ^{a)}	$X_{c,PLA}$ [%]
100/0	60.7	111.1	28	148.9 155.4	28	0.0
100/0 A	43.9	99.6	32	140.6 151.4	33	1.8
75/25	59.0	104.7	25	146.8 154.3	28	3.1
75/25 A	59.2	107.7	24	147.5 154.6	25	4.7
50/50	59.8	110.5	23	148.2 154.9	26	3.2
50/50 A	60.2	111.3	26	148.3 154.9	25	0.0
25/75	57.9	107.0	31	146.9 154.8	36	4.9
25/75 A	60.3	109.9	14	147.9 154.9	17	0.0
0/100 ^{b)}	–	–	–	122.4	11	–
0/100 A ^{b)}	–	–	–	111.0	8	–

^{a)}Transitions corresponding to PLA fraction; ^{b)}Melting endotherm values corresponding to pure PBAT.

Table 1 shows that the values of the cold crystallization enthalpy for the PLA rich phase are very close to that of the melting enthalpy. In the case of neat PLA, these two values are identical; hence the material was not able to crystallize during the previous cooling from the melt, only during the heating process from the glassy state.

In the case of the blends, the low values of the degree of crystallinity of the PLA rich phase indicate that the melting peak of the PLA fraction observed is mainly attributable to the fusion of crystals that are formed by cold-crystallization during the heating scan. When the PBAT plasticizer is added to the blends with PLA as the major phase there is a small increase of X_c . This might indicate that a small amount of material is able to crystallize during the previous cooling from the melt or it could be an error because of the underestimation of ΔH_{cc} , as indicated above.

The melting peak of the PLA rich phase shows two endothermic peaks. Separate experiments (not shown) performed at higher heating rates indicated that the second peak tends to disappear as the heating rate increases. Therefore, the two peaks seen in Figure 4 are a result of melting and re-crystallization processes that can occur during the heating scan. The first peak corresponds to the melting of the thinner crystals formed during

cold-crystallization that, upon heating, experience a complex melting and re-crystallization process to form more stable crystals (i.e., thicker crystals) that melt at higher temperatures. Yasuniwa et al.^[20] among others, have previously found similar results with PLA.

A decrease in the T_g of the PLA component as the amount of PBAT increases was found for the blends (the maximum drop in T_g detected was 3.8 °C, see Table 1). If the blends were immiscible, such a change would not be seen. Therefore, this decrease (albeit small) is a sign that there is a small amount of PBAT that can dissolve in the PLA, forming a PLA rich fraction (and concomitantly a PBAT rich fraction), indicating that the blends might be partially miscible. A drop in the cold-crystallization temperature (T_{cc}) and a small depression of the melting temperature of the PLA (T_m) fraction was also detected in some cases (see Table 1). Melting point depression is another indicator of partial blend miscibility, while a shift in the cold crystallization temperature could indicate a possible transference of impurities from the PBAT rich phase, allowing the PLA rich phase to crystallize at lower temperatures during heating.

Figure 5 shows a plot of the glass transition temperature corresponding to the PLA rich phase of the PLA/PBAT blends, as a function of composition. These values were obtained from two different techniques: DSC and DMA

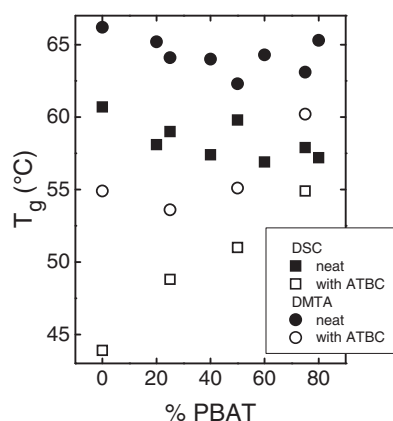


Figure 5. Comparison between the glass transition temperature values obtained by DMA and DSC for the PLA/PBAT blends with and without ATBC.

(see Table 1 and Table 2). The T_g values reported from DMA were the ones obtained from the $\tan\delta$ vs. temperature plots. Both techniques showed the same tendency of a slight decrease in the T_g of the PLA fraction as the amount of PBAT increases in the blends without plasticizer. Therefore, both techniques show that the blends probably exhibit some partial miscibility.

ATBC acts as a plasticizer for PLA, as shown in Table 1 and Figure 5, where the T_g value of neat PLA is reported to drop from 60.7 to 43.9 °C with the addition of ATBC. Figure 5 also shows that for the blends with ATBC, the plasticizing effect on the PLA rich phase practically disappears. DMA experiments showed a decrease in the T_g of neat PBAT when ATBC was added (see Figure 6). In the case of the blends with ATBC, they contain 10% of this additive with respect to the amount of PLA in the blends (see Experimental Section). Therefore, the lack of ATBC plasticization to the PLA rich phase in the blends

Table 2. Glass transition temperature of the PLA and PBAT rich phases determined by the $\tan\delta$ DMA curves.

PLA/PBAT	T_g PBAT [°C]	T_g PLA [°C]
0/100	-27.2	—
0/100 A	-36.8	—
25/75	-26.2	63.1
25/75 A	-30.5	60.2
50/50	-31.6	62.3
50/50 A	-38.1	55.1
75/25	-27.9	64.1
75/25 A	-45.0	53.6
100/0	—	66.2
100/0 A	—	54.9

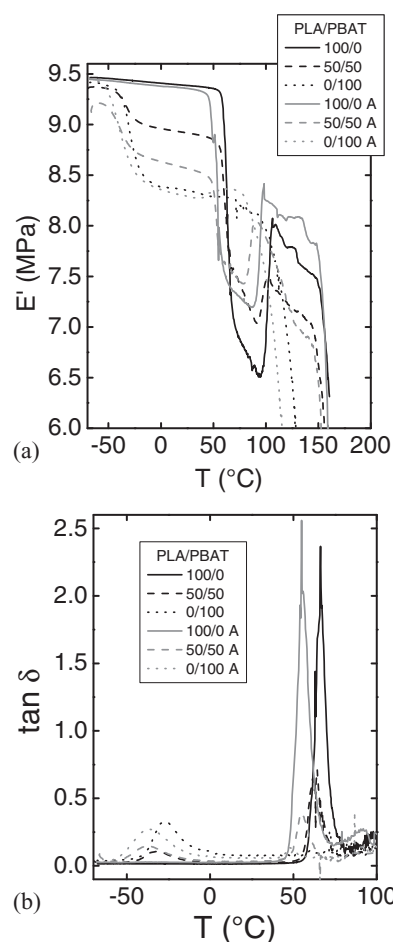


Figure 6. Variation of the (a) storage modulus and (b) $\tan\delta$ with temperature of the PLA/PBAT blends: 0/100, 50/50, 100/0, with and without ATBC.

can be explained by considering that ATBC has been preferentially dissolved in the PBAT rich phase (also, as the amount of PBAT increases, the amount of ATBC in the blends decreases). This is confirmed by DMA measurements reported in Table 2, where the T_g of the PBAT phase is seen to decrease upon addition of ATBC.

Figure 6 shows the variation of the storage modulus (E') and $\tan\delta$ as a function of temperature, obtained by DMA. In the case of neat PLA, the storage modulus exhibits a large drop at the T_g value of the material when the sample goes from the glassy to the rubbery state. At even higher temperatures (at around 100 °C) cold crystallization occurs and the modulus rises in view of the presence of the newly formed crystals. When these crystals melt at higher temperatures the modulus finally drops to very low values characteristic of the liquid state. Similar traces, only scaled according to their PLA content, can be seen for the blends. In addition, in the blends, the T_g of the PBAT rich phase can also be observed. However, as shown in Table 2, the T_g values for the PBAT rich phase did not vary

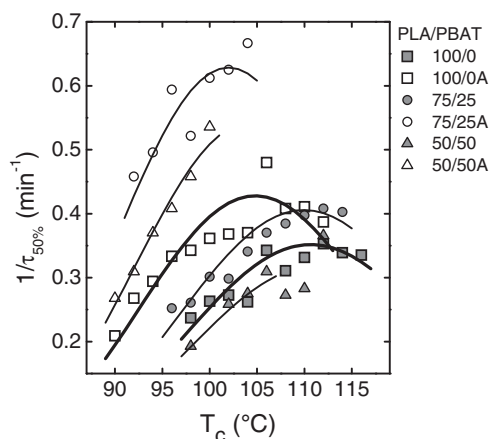


Figure 7. Overall crystallization as a function of the crystallization temperature of the PLA/PBAT blends with and without ATBC. Continuous lines correspond to the theoretical prediction of the Lauritzen–Hoffman theory.

significantly with composition except for the 50/50 blend where the value decreased as compared to neat PBAT.

Figure 7 shows the overall crystallization rates (expressed as the inverse of the normalized half-crystallization times determined by isothermal DSC experiments) as a function of the crystallization temperature T_c . The continuous lines are the theoretical predictions of the Lauritzen–Hoffman (L-H) nucleation and growth theory. We assumed that the crystallization takes place in regime II. For regime II, the L-H theory predicts that the growth rate can be approximated to:^[21]

$$G(T) = G_0 \exp\left(\frac{-U^*}{R(T_c - T_\infty)}\right) \exp\left(\frac{-K_g}{T_c \Delta T f}\right) \quad (2)$$

where $G(T)$ is the growth rate as a function of the temperature, G_0 is a constant of growth rate, U^* is the activation energy needed to move chains to a growing nucleus, R is the universal gas constant, T_c is the crystallization temperature, T_∞ is the temperature at which there is no more chain mobility, K_g is the secondary nucleation constant, ΔT is the supercooling and f is a factor of temperature correction calculated by the following equation 3:^[21]

$$f = \frac{2T_c}{T_c + T_m^0} \quad (3)$$

In the case of data collected by DSC, the crystallization kinetics contains contributions from both nucleation and growth, and in Equation 2, $G(T)$ can be substituted by the inverse of the half-crystallization time as reported by Lorenzo and Müller.^[22] This approach can be controversial. As pointed out previously by Lorenzo and Müller, the fitting parameters can only be exactly equivalent to those obtained using spherulitic growth rate data, when the

nucleation step is essentially instantaneous. They demonstrated that if self-nucleation is performed before determining the overall isothermal crystallization kinetics by DSC, then the K_g parameter obtained is identical to that determined by applying the L-H treatment to spherulitic growth rate data (see Lorenzo and Müller^[22] and references therein). When the nucleation varies with the experimental crystallization temperature employed, then the inverse of the half-crystallization time is a complex quantity that contains variable nucleation and growth contributions. Pluta and Galeski^[23] found in PLA samples that were cold-crystallized isothermally that the nucleation density was a function of T_c and that it is higher than in the case of the samples crystallized from the melt. Nevertheless, the fitting can still be performed with the knowledge that the required free energy for nucleation and growth will be higher than that for spherulite growth only. Hence, we expect the K_g values determined by the application of the L-H treatment to DSC data to be higher than that obtained from spherulitic growth only. Regarding the dependence of the overall crystallization rates obtained by DSC as a function of T_c shown in Figure 7, all blends show signs of the typical bell-shaped curve expected, which means that the overall crystallization process is governed by molecular diffusion at low temperatures and by primary and secondary nucleation at high crystallization temperatures.^[24] The experimental data matched the L-H prediction at low T_c values before the maxima in crystallization rate.

Even though the data in Figure 7 is noisy, there are changes in the overall crystallization rate with PBAT addition which could be attributed to changes in nucleation density caused by impurities transfer, as already stated above (and as it will be corroborated below, when the polarized optical microscopy results are presented), or by possible blend miscibility. These changes are magnified when the ATBC is added.

The addition of ATBC clearly raises the rate of overall crystallization as a result of the increase in the molecular mobility caused by the plasticization process. For the same reason the plot in Figure 7 is also shifted to lower crystallization temperatures, since the plasticized chains will require a higher supercooling to crystallize.

Neat PLA is plasticized by ATBC and its crystallization rate is increased, as shown in Figure 7 (compare the data for 100/0 and 100/0A samples), as expected. However, the combination of PBAT as a dispersed phase and the addition of ATBC displayed a remarkable synergistic effect in terms of overall crystallization rate. This synergy has a complex dependence with PBAT addition. The PLA rich phase within the 75/25 blend with ATBC exhibits a larger increase in overall crystallization kinetics than that exhibited by the 100/0A material or the 50/50A. It must be noted that

Table 3. Parameters of the Avrami fit obtained from the crystallization of the PLA rich phase in the PLA/PBAT blends, for different crystallization temperatures (T_c): Avrami exponent (n), predicted half-time crystallization ($t_{1/2\text{theo}}$), experimental half-time crystallization ($t_{1/2\text{exp}}$), overall transformation constant (k) and the data correlation coefficient (R^2). A = ATBC.

Blend	T_c [°C]	n	$t_{1/2\text{theo}}$ [min]	$t_{1/2\text{exp}}$ [min]	k [min ⁻ⁿ]	R^2	Blend with plasticizer	T_c [°C]	n	$t_{1/2\text{theo}}$ [min]	$t_{1/2\text{exp}}$ [min]	k [min ⁻ⁿ]	R^2
100/0	98	2.4	4.29	4.22	0.0163	0.99986	100/0 A	90	2.9	4.98	4.78	0.0062	0.99995
	102	2.6	3.72	3.67	0.0167	0.99987		94	2.8	3.55	3.40	0.0204	0.99987
	106	3.0	2.95	2.92	0.0325	0.99985		98	3.1	2.97	2.92	0.0241	0.99997
	110	3.3	3.00	3.02	0.0146	0.99994		102	3.7	2.72	2.72	0.0176	0.99998
	114	3.4	2.96	2.95	0.0123	0.99991		106	3.0	2.16	2.08	0.0702	0.99962
	116	3.5	3.01	2.98	0.0151	0.99998		112	3.7	2.60	2.58	0.0201	0.99991
75/25	96	2.4	4.08	3.97	0.0244	0.99985	75/25 A	92	3.4	2.25	2.18	0.0442	0.99978
	100	2.6	3.39	3.32	0.0275	0.99981		94	3.4	2.05	2.02	0.0591	0.99986
	104	3.0	2.95	2.93	0.0257	0.99999		96	3.3	1.73	1.68	0.1110	0.99978
	108	3.3	2.61	2.60	0.0296	0.99992		100	3.8	1.67	1.63	0.0980	0.99969
	112	3.4	2.46	2.45	0.0335	0.99993		102	3.5	1.66	1.60	0.1155	0.99911
	114	3.5	2.49	2.48	0.0294	0.99994		104	3.6	1.54	1.50	0.1454	0.99943
50/50	98	2.9	5.17	5.18	0.0057	1.00000	50/50 A	90	3.0	3.86	3.73	0.0114	0.99974
	102	2.9	3.84	3.87	0.0146	0.99999		92	3.3	3.28	3.23	0.0144	0.99996
	104	3.1	3.58	3.63	0.0133	1.00000		94	3.0	2.78	2.70	0.0315	0.99982
	106	3.1	3.20	3.23	0.0191	0.99999		96	3.3	2.47	2.45	0.0358	0.99996
	110	2.7	3.82	3.53	0.0182	0.99972		98	3.6	2.18	2.18	0.0437	1.00000
	112	3.2	2.73	2.73	0.0288	0.99999		100	3.2	1.91	1.87	0.0901	0.99999

the isothermal crystallization of the PLA/PBAT 25/75 blend was not studied since the crystallization started before the isothermal T_c was reached in the calorimeter. This result means that the crystallization of the PLA rich phase within the 25/75 PLA/PBAT phase (with or without ATBC) was faster than that of all the other blends, thus confirming the complex trend with PBAT and ATBC addition.

To analyze the isothermal crystallization kinetics, the Avrami equation was used following the procedure developed by Lorenzo et al.^[25] The Avrami equation can be written as the following equation 4:^[25–28]

$$1 - V_c(t - t_0) = \exp(-k(t - t_0)^n) \quad (4)$$

where V_c is the relative volumetric transformed fraction as a function of the experimental time (t), t_0 is the induction time, k is the overall crystallization rate constant, and n is the Avrami index.

The Avrami theory was applied to fit the isothermal DSC data using a convenient conversion range between 3 and 20% where the fitting is normally excellent and unaffected by initial fluctuations in the isothermal exothermic data or by secondary crystallization (see Lorenzo et al.^[25]). Table 3 shows the values of the Avrami fitting

parameters such as the Avrami index (n), the overall crystallization rate constant (k) and the predicted half crystallization time ($t_{1/2\text{theo}}$) as compared to the experimental values ($t_{1/2\text{exp}}$).

The values of the overall crystallization rate constant exhibited trends that are compatible with those displayed by the half-crystallization times, once its dependence with the Avrami index is taken into account (i.e., for instance if the values of k are elevated to the power $1/n$, then they could all be expressed as min^{-1} and can be easily compared with one another).

The half crystallization times predicted by the Avrami fit are in full agreement with the experimental values indicating that for at least up to 50% conversion to the crystalline state the Avrami equation can predict the overall crystallization process. We found that the Avrami equation fitted remarkably well most of the overall crystallization kinetics process well past the primary crystallization stage. The goodness of the fit can be observed in Figure 8 where the DSC traces predicted by the Avrami fits are compared with the experimental isothermal scans.

Table 3 reports the values of the Avrami index of the PLA/PBAT blends with and without plasticizer for all the crystallization temperatures studied. The increase of n with the crystallization temperature is typical of

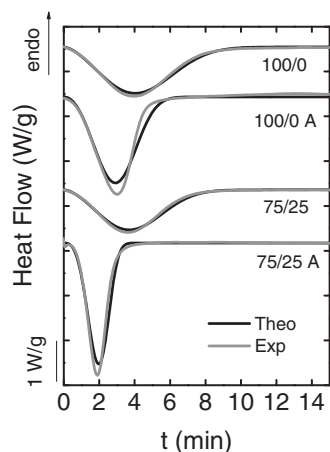


Figure 8. Comparison of sample DSC isothermal scans obtained experimentally and predicted by the Avrami equation for the PLA/PBAT blends ($T_c = 98$ °C).

crystallizable polymers, since the nucleation becomes more sporadic as T_c increases.^[29] Most n values are close to three indicating that instantaneous spherulites are formed when the material crystallizes by isothermal cold-crystallization.

Extrapolated values of T_m^0 were calculated employing the Hoffman–Weeks plot (results not shown). As it can be seen in Figure 9, after the samples were isothermally crystallized, their heating scans were recorded in the DSC. All samples displayed two melting peaks. The second melting peak is attributable to reorganization during the scan and its value does not change with T_c , so it cannot be employed to calculate T_m^0 . With the T_m values of the first melting peak, we employed the Hoffman–Weeks plot and we found values ranging from 159.2 to 161.7 °C for the

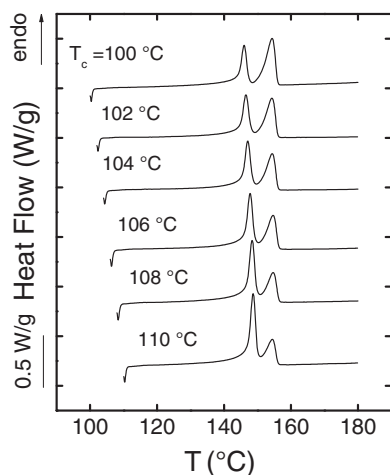


Figure 9. DSC heating scans for neat PLA after isothermal crystallization at several temperatures.

blends and neat PLA with and without plasticizer (there was no significant change in T_m^0 with composition).

The values of T_m^0 found here are significantly lower than others reported in the literature (206.8 °C).^[30] Tsuji and Ikada^[31] obtained lower values of T_m^0 for PLLA films that were annealed without deleting the thermal history of the samples and higher values when the thermal history of the films was erased. Pluta and Galeski^[23] performed isothermal crystallization of PLA from the melt and also by heating the samples from the glassy state to allow isothermal cold crystallization and found that there were differences in spherulite sizes, but the lamellar features and the melting behavior of the crystals were similar regardless of the crystallization method. One possible explanation for the lower values of T_m^0 obtained could be related to the content of the D-stereoisomer in the PLA employed here (as argued by Masirek et al.^[32]). Since this is a commercial sample it will not be 100% pure poly(L-lactide).

The bimodal melting shown in Figure 9 after isothermal crystallization was further analyzed by integrating the areas under each peak (see Figure 10). As can be seen in Table 4 the melting temperature of the first peak increases with crystallization temperature, which indicates that thicker lamellar crystals are formed at higher T_c , as expected. The melting temperature of the second peak does not show significant changes with T_c . This is consistent with the fact that the second melting peak is the product of the melting of crystals that were formed during heating (i.e., during a process of partial melting and re-crystallization during the heating DSC scan) and therefore its melting peak will be constant since its peak temperature is an exclusive function of the constant heating rate employed.

In all cases, Figure 10 shows that there is an increase in the area of the first peak with crystallization temperature, and a corresponding decrease in the area of the

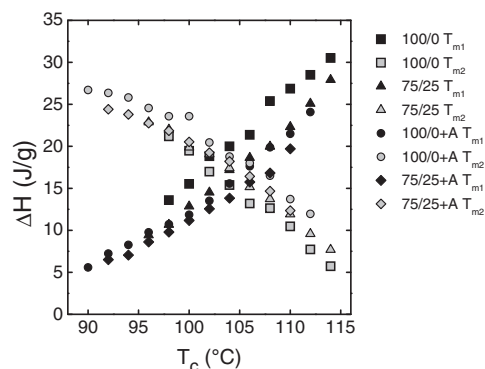


Figure 10. Values of the partial melting peak area enthalpies (from Figure 9) of the PLA/PBAT blends as a function of the isothermal crystallization temperature.

Table 4. Melting peak temperature and partial enthalpies of the double melting peaks of neat PLA after isothermal crystallization.

T_c [°C]	1st Peak		2nd Peak	
	T_m [°C]	ΔH_m [J g ⁻¹]	T_m [°C]	ΔH_m [J g ⁻¹]
98	145.4	14	154.2	21
100	146.0	16	154.3	19
102	146.5	19	154.4	17
104	147.1	20	154.3	15
106	147.8	21	154.7	13
108	148.4	25	154.5	13
110	148.7	27	154.6	10
112	149.3	29	154.1	8
114	149.6	31	154.1	6
116	150.2	33	153.8	3

second peak. By raising the isothermal crystallization temperature more thermodynamically stable crystals are formed since they will possess thicker lamellae. The consequence of this is that a lower extent of melting–recrystallization during heating will take place after the

isothermal crystallization. This explains the decrease in the melting enthalpy of the second melting peak, and the consequent increase in the melting enthalpy of the first melting peak.

There seems to be a decrease in the melting enthalpy when ATBC and PBAT are added to the PLA matrix, whether they are added together or separately. Even though the rate of crystallization is increased when these materials are present in the blends, apparently the absolute amount of material that crystallizes during the isothermal process decreases.

Figure 11 shows the spherulitic morphology of the PLA/PBAT blends with and without plasticizer. The spherulites (whose sign was negative as expected for PLA) observed correspond to PLA superstructures that crystallized from the melt. It was not possible to observe the spherulite growth of the PBAT at an appropriate magnification. The droplets observed in the melt surrounding the spherulites indicate that there are two phases in the molten state. Nevertheless, some droplets can be seen inside the spherulites of the blends with PBAT, possibly indicating that a molten PBAT rich phase is trapped within the spherulitic superstructure. Occlusion by one phase of the spherulites of another phase is a behavior commonly seen in blends that are partially miscible.^[33] However, the

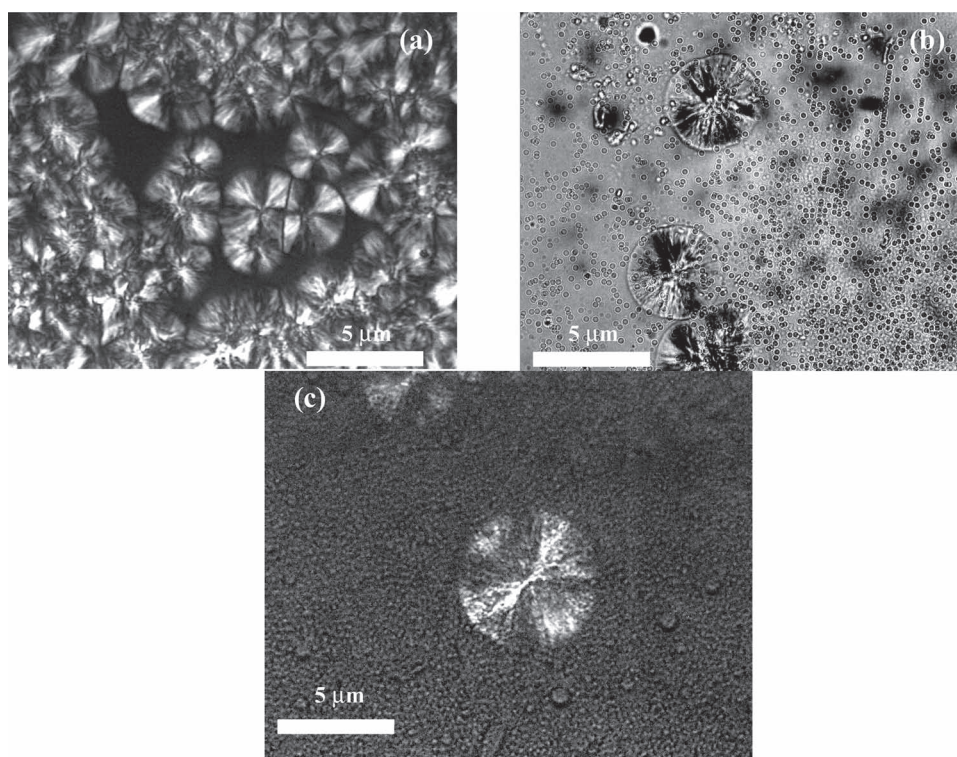


Figure 11. Spherulitic morphology of the PLA/PBAT blends observed by POM, at a crystallization temperature of 120 °C. a) 100/0, b) 100/0 +ATBC, and c) 75/25.

Table 5. Apparent nuclei density of PLA spherulites observed by POM in the PLA/PBAT blends, crystallized at various temperatures (T_c).

PLA/PBAT	T_c [°C]	Apparent nuclei density [units μm^{-2}]
100/0	120	0.130
	125	0.044
	130	0.025
	135	0.002
	140	0.002
75/25	115	0.046
	120	0.004
	140	0.002
100/0 A ^{a)}	110	0.246
	115	0.099
	120	0.008

^{a)}A = ATBC.

effect was also observed for some immiscible polymer blends. Bartczak et al.^[34] reported that in the case of iPP/rubber blends, inclusion of rubber droplets were found in the iPP spherulites and it was concluded that the interfacial energy difference between the melt and solid rubber has an influence on the processes of occlusion, deformation, or rejection of dispersed particles from the crystallization front.

To study the effect of the presence of PBAT on the nucleation of the PLA spherulites, we determined an apparent nucleation density by PLOM as shown in Table 5. We employed the images collected for spherulitic growth rate measurements and assumed that each spherulite had been grown from one nucleus. As the crystallization temperature decreases the apparent density increases as can be seen in the micrographs, indicating that in the range of crystallization temperatures studied, the nucleation rate increases with supercooling when the crystallization is performed from the molten state. By adding either 25% PBAT or 10% ATBC, a drastic drop in nuclei density occurs. In the first case, this drop indicates that the nucleation rate is decreased by the presence of PBAT, a fact that could be related to impurities transfer from PLA to PBAT (a similar result was found for cold crystallization in Figure 4). In the second case, the addition of ATBC decreases the nucleation rate at high temperatures because of the increased mobility of the PLA chains as a direct consequence of plasticization.

The spherulite growth rates (G) of PLA/PBAT blends without plasticizer and of PLA with ATBC are shown in Figure 12 as a function of the crystallization

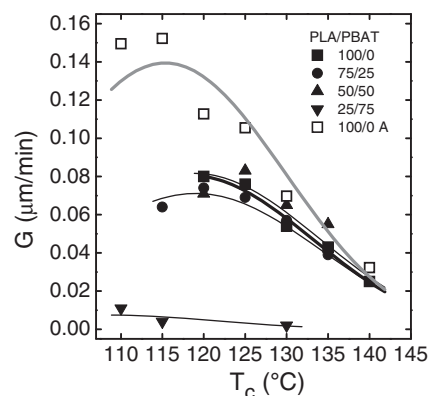


Figure 12. Spherulitic growth rate as a function of crystallization temperature of the PLA/PBAT blends.

temperature. When PBAT is the minor phase, no significant changes in spherulite growth were detected. Nevertheless, G is largely affected when the blend contains 75% PBAT. When blends are totally immiscible, the growth rate of the crystals formed by the crystallizable phase remains largely unaffected by the presence of the second phase, at least in the composition range employed here. Nevertheless, even in immiscible blends, the growth rate of the crystallizable phase could be affected by the second phase as mentioned earlier, because of the superficial energy differences between both polymers during spherulitic growth. However, considering that the change observed here is rather large (i.e., when the change from 100/0 to the 25/75 PLA/PBAT blend is considered in Figure 12) and also the evidences gathered so far (small changes in T_g and T_m and the occlusion of one phase on the other), we believe the blends could be displaying signs of partial miscibility.

Figure 12 also shows that since the spherulitic growth rate showed little change with PBAT content for PBAT contents equal to or lower than 50%, the variations seen in the overall crystallization rate in that composition range (Figure 7) are mainly attributable to changes in the nucleation rate.

Table 6 shows the parameters obtained by the L-H fit to the data presented in Figure 7 and in Figure 12. Both nucleation and growth contribute to the K_g^τ values (where the superscript indicates that values of the inverse half-crystallization time were employed as average overall crystallization rate values obtained by DSC), whereas only growth contributes to the values of K_g^G (the superscript indicates that spherulite growth rate values were employed as average growth rates in Equation 2, see Lorenzo and Müller^[22]).

The values reported in Table 6 indicate that in all comparable cases (i.e., same samples) the values of K_g^τ are

■ Table 6. Parameters obtained by fitting the L-H equation to the crystallization of the PLA/PBAT blends, determined by DSC and PLOM.

DSC							
% PBAT	Additive	$1/\tau_0 (\times 10^9) [s^{-1}]$	$\sigma [\text{erg cm}^{-2}]$	$\sigma_e [\text{erg cm}^{-2}]$	$q (\times 10^{-12}) [\text{erg}]$	$K_g^\tau [K^2]$	R^2
0	s/a	3.60	9.79	170.4	2.23	588 075	0.99466
	ATBC	1816.05	9.79	228.8	3.00	789 800	0.99212
25	s/a	7.96	9.79	176.6	2.31	609 467	0.99407
	ATBC	9814.46	9.79	264.7	3.47	913 464	0.98671
50	s/a	1.88	9.79	165.1	2.16	569 955	0.96128
	ATBC	4206.66	9.79	234.8	3.08	810 341	0.99089
PLOM							
		$G_0 [\text{cm s}^{-1}]$	$\sigma [\text{erg cm}^{-2}]$	$\sigma_e [\text{erg cm}^{-2}]$	$q (\times 10^{-12}) [\text{erg}]$	$K_g^G [K^2]$	R^2
0	s/a	262.8	9.89	113.2	1.518	403 375	0.99773
	ATBC	3008.2	9.89	129.9	1.748	462 938	0.99041
25	s/a	136.9	9.89	108.6	1.458	387 042	0.99705
50	s/a	176.9	9.89	109.6	1.47	390 707	0.97682
75	s/a	56086	9.89	183.4	2.46	653 753	0.93462

higher than K_g^G . These results are in agreement with the fact that PLOM only deals with spherulite growth and therefore the energy barrier for growth only should be lower than the energy barrier for both primary and secondary nucleation (or nucleation and growth, as determined by DSC), in agreement with the findings of Lorenzo and Müller.^[22] The values of K_g can be considered proportional to these energy barriers.

Table 6 also reports other parameters that vary in the same way as the K_g values. The fold surface free energy is also higher for overall crystallization than for growth only. In an analogous way, the work needed for the chains to undergo folding (q values) follows the same trend.

The K_g , σ_e , and q values were nearly independent of blend composition except for the case of the 25/75 PLA/PBAT blend, where a large increase was observed in view of the difficulties experienced by the PLA rich phase to grow its spherulites (Figure 12).

The addition of ATBC caused an increase in the K_g^τ values, a fact probably attributable to its ability to decrease the nucleation rate (see Table 5 and Figure 12).

4. Conclusion

The PLA/PBAT blends showed a two-phase morphology for all the compositions examined here. Nevertheless, we collected evidence that could indicate a partial miscibility between the blend components that lead us to believe that two phases coexist: a PLA rich phase and a

PBAT rich phase, even if the composition of the phases only includes a very limited amount of the second component. The collected evidence that indicate partial miscibility is: 1) a shift in the glass transition temperature of the PLA rich phase with PBAT addition, as detected by both DSC and DMA techniques; 2) a very small but reproducible decrease in T_m values for the PLA phase in the blends; 3) changes in the spherulitic growth rate with blend composition; 4) occlusions of PBAT within the PLA spherulites.

ATBC was able to plasticize both neat PLA and PBAT (as indicated by decreases in T_g and increases in crystallization rate). In the case of the blends, it seems that ATBC prefers to be included within the PBAT rich phase rather than within the PLA rich phase. There is a synergistic effect on the overall crystallization rate of the PLA component when both PBAT and ATBC are added to PLA, as shown by an increase in the overall crystallization rate when compared to the rates obtained for the blends when these two are added separately to the PLA matrix.

Acknowledgements: The USB team acknowledges funding by Decanato de Investigación y Desarrollo through grant USB-DID-GID-02. The IPCF-CNR team also acknowledges funding by MIUR through grant PRIN 2008 Prot. 200898KCKY.

Received: July 28, 2011; Revised: October 2, 2011; Published online: December 12, 2011; DOI: 10.1002/macp.201100437

Keywords: isothermal crystallization; poly(lactic acid); poly(butylene adipate-co-terephthalate); thermal properties.

- [1] M. B. Coltelli, I. Della Maggiore, M. Bertoldo, F. Signori, S. Bronco, F. Ciardelli, *J. Appl. Polym. Sci.* **2008**, *110*, 1250.
- [2] L. Jiang, M. P. Wolcott, J. Zhang, *Biomacromolecules* **2006**, *7*, 199.
- [3] H. Xiao, W. Lu, J.-T. Yeh, *J. App. Polym. Sci.* **2009**, *112*, 3754.
- [4] C. K. Williams, M. A. Hillmyer, *Polym. Rev.* **2008**, *48*, 1.
- [5] Z. Kulinski, E. Piorkowska, *Polymer* **2005**, *46*, 10290.
- [6] M. Baiardo, G. Frisoni, M. Scandola, M. Rimelen, D. Lips, K. Ruffieux, E. Wintermantel, *J. Appl. Polym. Sci.* **2003**, *90*, 1731.
- [7] I. Pillin, N. Montrelay, Y. Grohens, *Polymer* **2006**, *47*, 4676.
- [8] L. V. Labrecque, R. A. Kumar, V. Davé, R. A. Gross, S. P. McCarthy, *J. Appl. Polym. Sci.* **1997**, *66*, 1507.
- [9] N. Ljungberg, B. Wesslén, *Polymer* **2003**, *44*, 7679.
- [10] H. Xiao, W. Lu, J.-T. Yeh, *J. App. Polym. Sci.* **2009**, *113*, 112.
- [11] H. Tsuji, H. Takai, S. K. Saha, *Polymer* **2006**, *47*, 3826.
- [12] M. Shibata, Y. Inoue, M. Miyoshi, *Polymer* **2006**, *47*, 3557.
- [13] J. T. Yeh, C. J. Wu, Ch. Tsou, W. L. Chai, J. D. Chow, C. Y. Huan, K. N. Chen, C. S. Wu, *Polym. Plast. Tech. Eng.* **2009**, *48*, 571.
- [14] D. Newman, E. Laredo, A. Bello, A. Grillo, J. L. Feijoo, A. J. Müller, *Macromolecules* **2009**, *42*, 5219.
- [15] M. Hiljanen-Vainio, P. Vapormaa, J. Seppala, P. Tormala, *Macromol. Chem. Phys.* **1996**, *197*, 1503.
- [16] M. E. Broz, D. L. VanderHart, N. R. Washburn, *Biomaterials* **2003**, *24*, 4181.
- [17] H. Tsuji, Y. Ikada, *J. App. Polym. Sci.* **1996**, *60*, 2367.
- [18] F. Signori, M. B. Coltelli, S. Bronco, F. Ciardelli, *Polym. Degr. Stab.* **2009**, *94*, 74.
- [19] M. B. Coltelli, C. Toncelli, F. Ciardelli, S. Bronco, *Polym. Degrad. Stab.* **2011**, *96*, 982.
- [20] M. Yasuniwa, S. Tsubakihara, Y. Sugimoto, C. Nakafuku, *J. Polym. Sci., Part B: Polym. Phys.* **2003**, *42*, 25.
- [21] J. I. Lauritzen Jr., J. D. Hoffman, *J. App. Phys.* **1973**, *44*, 4340.
- [22] A. T. Lorenzo, A. J. Müller, *J. Polym. Sci., Part B: Polym. Phys.* **2008**, *46*, 1478.
- [23] M. Pluta, A. Galeski, *J. Appl. Polym. Sci.* **2002**, *86*, 1386.
- [24] B. Wunderlich, *Thermal Analysis of Polymeric Materials*, Springer, Berlin **2005**.
- [25] A. T. Lorenzo, M. L. Arnal, J. Albuerno, A. J. Müller, *Polym. Test.* **2007**, *26*, 222.
- [26] M. J. Avrami, *Chem. Phys.* **1939**, *7*, 1103.
- [27] M. J. Avrami, *Chem. Phys.* **1940**, *8*, 212.
- [28] M. J. Avrami, *Chem. Phys.* **1941**, *9*, 177.
- [29] U. Gedde, *Polymer Physics*, Kluwer, Dordrecht **1995**.
- [30] R. Vasanthakumari, A. J. Pennings, *Polymer* **1983**, *24*, 175.
- [31] H. Tsuji, Y. Ikada, *Polymer* **1995**, *36*, 2709.
- [32] R. Masirek, Z. Kulinski, D. Chionna, E. Piorkowska, M. Pracella, *J. Appl. Polym. Sci.* **2007**, *105*, 255.
- [33] J. M. Schultz, *Polymer Crystallization, The Development of Crystalline Order in Thermoplastic Polymers*, American Chemical Society, New York **2001**.
- [34] Z. Bartczak, A. Galeski, E. Martuscelli, *Polym. Eng. Sci.* **1984**, *24*, 1155.